

Supplementary Appendix S1

Window sampling for training

As discussed in the Methods - Learning architecture and algorithm, for the training of the model, 50% of the data of each subject were used. The randomly sampling for this training data set was designed in a way so that N_B blocks with a length of $L_B = 30$ seconds windows were used. Thus, at first the number of the starting points N_B was calculated as $N_B = N_M / (2 \cdot L_B)$, where L_B can be converted in units of the number of measurements N_M considering the acquisition rate. As a next step, the random starting points were calculated by generating N_B random numbers in a range from 1 to N_W . That the network is not limited to learn features from blocks with a fixed length, all N_B blocks get randomly assigned a length of L'_B in a range L_B to $L_B + 20$ windows. The different blocks were allowed to overlap. The remaining windows are used for validation. The training data is then used to train the model and the obtained model can be used to predict the ICP of the validation data or the future subjects.

Supplementary Appendix S2

Benign enlargement of subarachnoid spaces cohort

This part of the supplementary material contains detailed information about the BESS cohort for further understanding of the data set. Given the small size of the cohort, we have checked whether a subject deviates the results with a systematic error. For this purpose, we have plotted a histogram showing the distribution of the measured ICP for each subject as well as time traces which show the ICP measured with an invasive sensor compared to the non-invasively estimated ICP.

Figure S1 shows the distribution of the measured ICP values for the 30 second binned data set for the whole infant cohort, to see if a subject dominates a certain range of ICP values compared to the overall distribution. The subjects are color coded. By looking at this figure it is clear that subject 1 and 6 are at the edges of the distribution and that other subjects do not show the same ICP values. Furthermore, the ICP values are not equally distributed.

Figure S2 shows basically the same information as Figure 3 in the main manuscript, however the subjects are color coded as in Figure S1, to see if the results are deviated by a certain subject.

For a qualitative illustration, Figures S3 to S8 show the time traces for each subject. Measurements from the epidural ICP sensor are marked by blue dots, while the grey (training) and red (validation) dots are the result of our machine learning algorithm prediction. The error bars represent the standard deviation of the 30 s bin. It can be seen that the trend of the predicted ICP follows the invasively measured ICP.

Supplementary Appendix S3

Traumatic brain injury cohort

This part of the supplementary material contains detailed information about the TBI cohort for further understanding of the data set. Given the small size of the cohort, we have checked whether a subject deviates the results with a systematic error. For this purpose, we have plotted a histogram showing the distribution of the measured ICP for each subject as well as time traces which show the ICP measured with an invasive sensor compared to the non-invasively estimated ICP.

The distribution of the obtained ICP values binned in 30 second windows is shown in Figure S9 for each subject of the TBI cohort, showing clearly different ICP values for the different subjects, which are not equally distributed. The subjects are color coded. The higher ICP values are driven by subject 3.

Figure S10 shows the same information as Figure 4 in the main manuscript, however the subjects are color coded as in Figure S9, to see if a subject deviates the results with a systematic error.

Again, time traces of the measured and predicted ICP are shown in Figures S11 to S18, where the blue dots represent the average over the 30 s bins of the real ICP with its standard deviation, whereas the grey (training) and red (validation) dots are derived from our algorithm. For measurements with a measurement time longer than one hour additionally a zoom of 30 minutes is shown to better visualize the data. These time traces demonstrate the ability to capture intrinsic dynamics, such as rises and falls, in the ICP time series. In Figure S13 a spontaneous increase and a decrease can be observed, while the predicted index follows the standard ICP measurement. In Figure S16 an increase in ICP was provoked by changing the head-of-bed position of the patient (see Methods - Clinical populations). In Figure S14 slow waves of the ICP signal are evident.

Supplementary figures

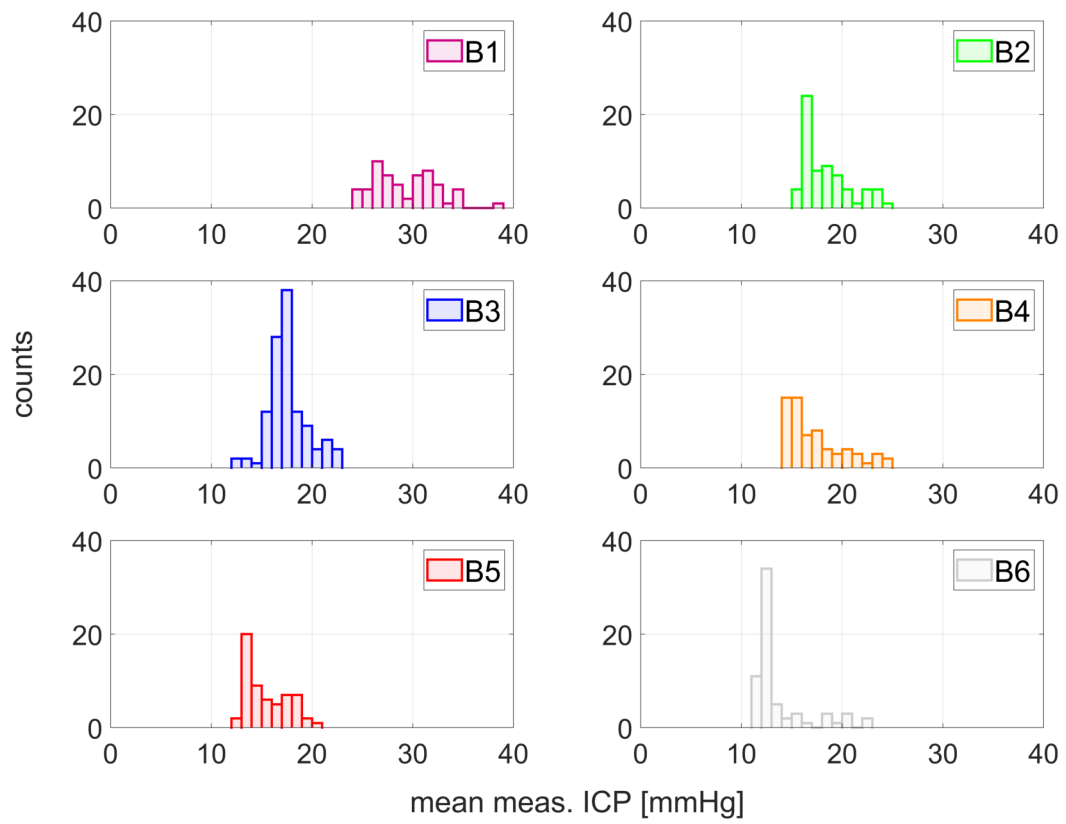


Figure S1: Distributions of the measured ICP values for each BESS cohort subject.

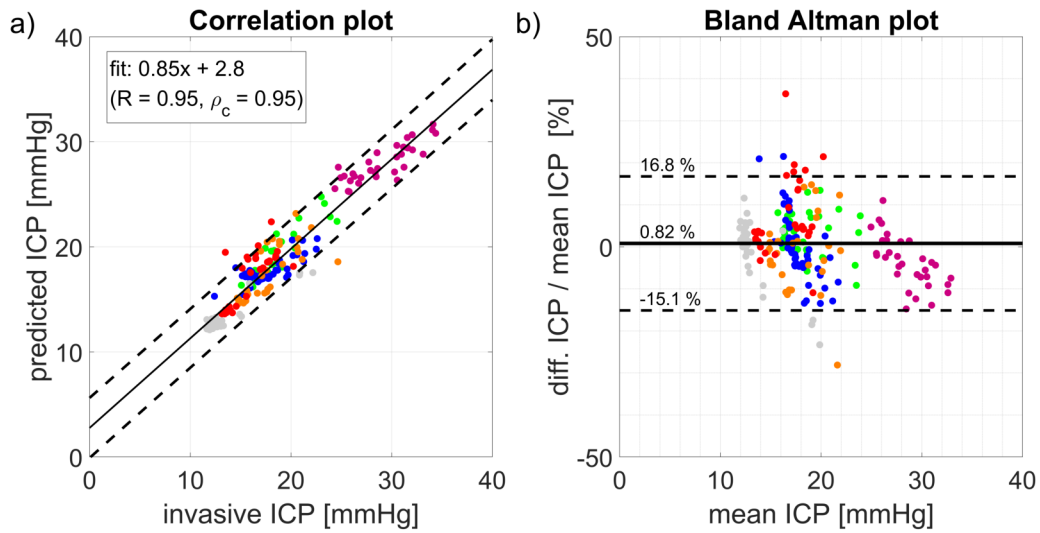


Figure S2: BESS cohort: The subjects are color coded as indicated in Figure S1, otherwise the plot contains the same info as Figure 3. Panel a) Correlation analysis. The solid line represents the best linear fit and the dashed lines the 95% confidence interval of the fit. Panel b) Bland-Altman plot. The solid line represents the mean (= bias) and the dashed lines the mean \pm 1.96 standard deviations. (mean ICP = mean of predicted ICP and invasive ICP, diff. ICP = predicted ICP - invasive ICP).

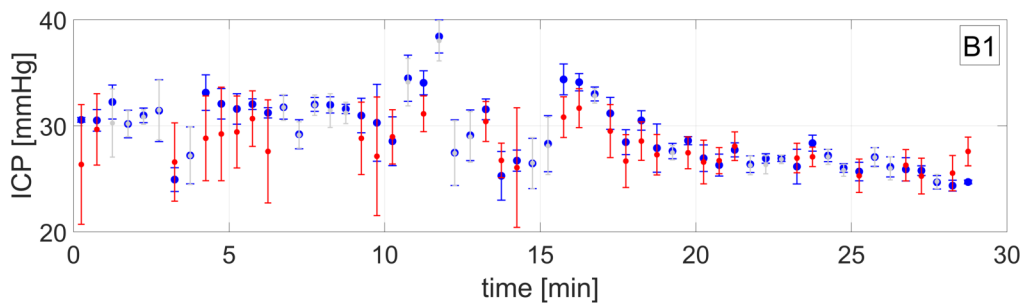


Figure S3: Time trace of BESS subject B1. The 30 second bins are plotted with its standard deviation. The blue dots represent the ground truth (invasive ICP) while the red dots are the predicted ICP values of the validation and the grey dots were used in the training.

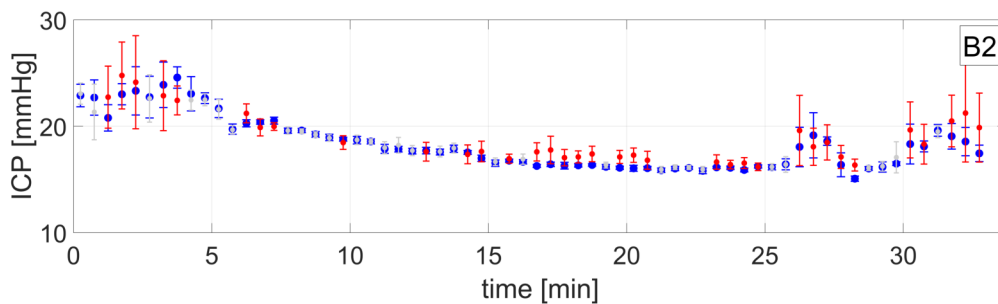


Figure S4: Time trace of BESS subject B2. The color scheme is the same as in Figure S3.

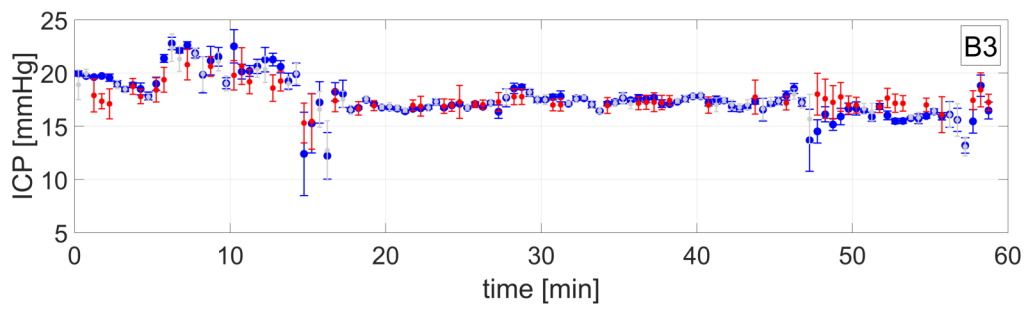


Figure S5: Time trace of BESS subject B3. The color scheme is the same as in Figure S3.

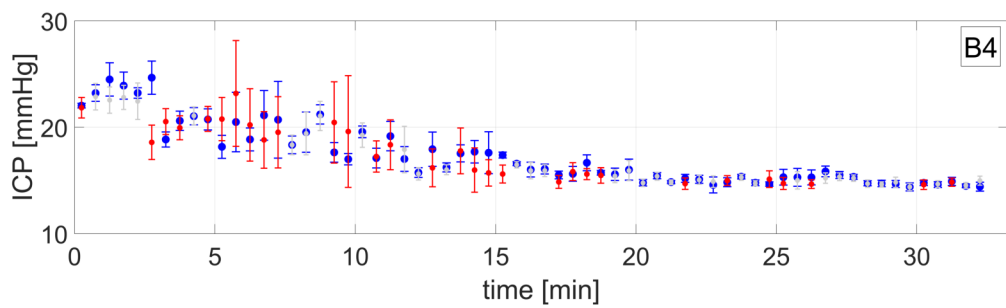


Figure S6: Time trace of BESS subject B4. The color scheme is the same as in Figure S3.

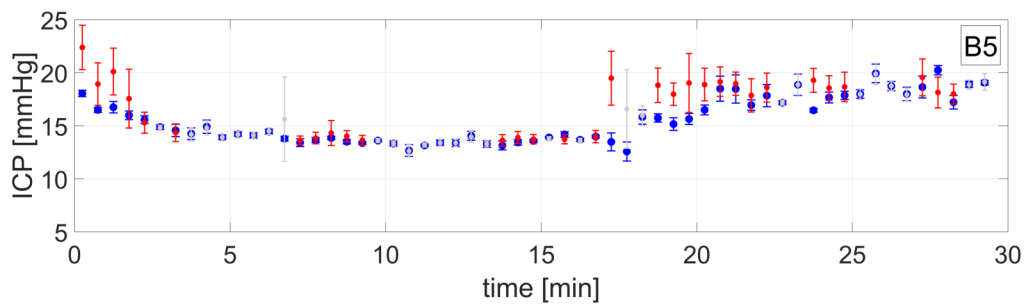


Figure S7: Time trace of BESS subject B5. The color scheme is the same as in Figure S3.

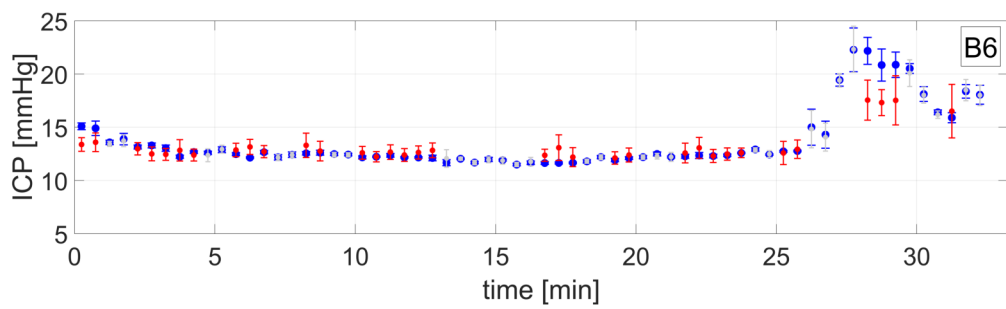


Figure S8: Time trace of BESS subject B6. The color scheme is the same as in Figure S3.

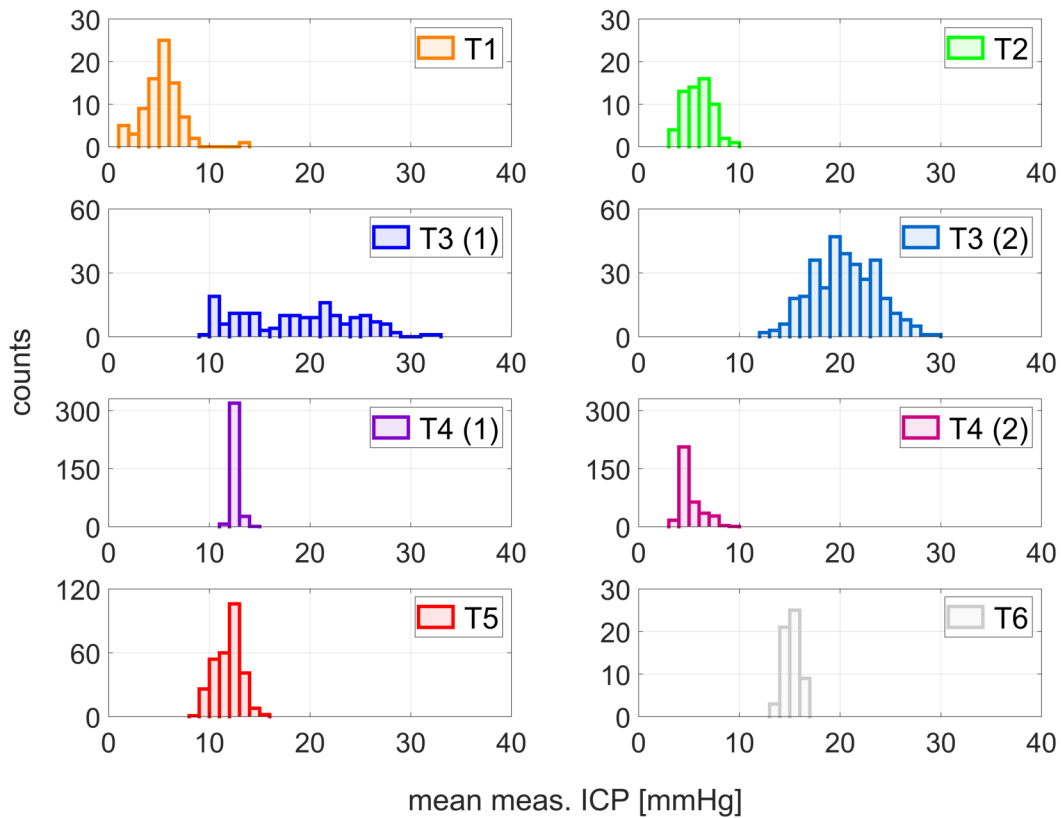


Figure S9: Distributions of ICP for each TBI cohort subject.

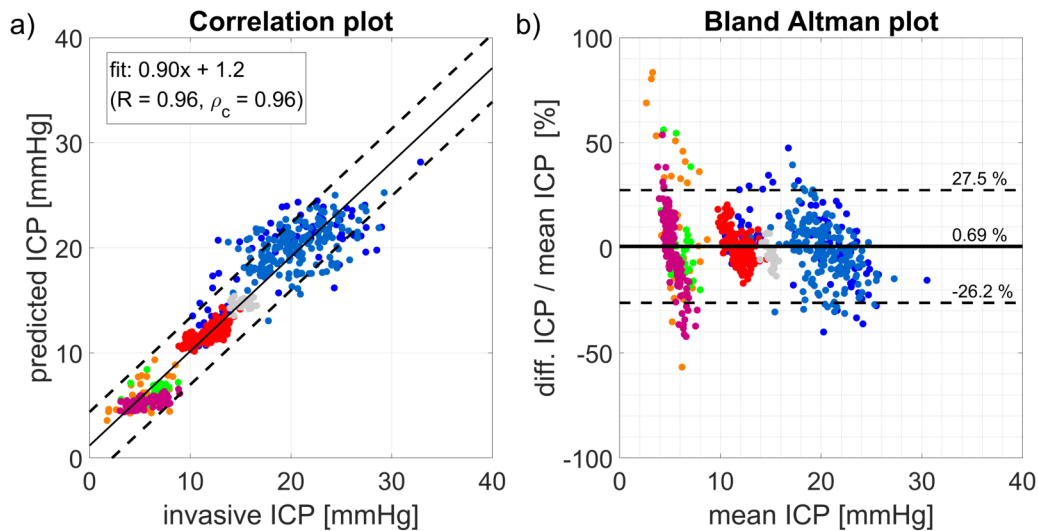


Figure S10: TBI cohort: The subjects are color coded as indicated in Figure S9, otherwise the plot contains the same information as Figure 4. Panel a) Correlation analysis. The solid line represents the best linear fit and the dashed lines the 95% confidence interval of the fit. Panel b) Bland-Altman plot. The solid line represents the mean (= bias) and the dashed lines the mean \pm 1.96 standard deviations. (mean ICP = mean of predicted ICP and invasive ICP, diff. ICP = predicted ICP - invasive ICP).

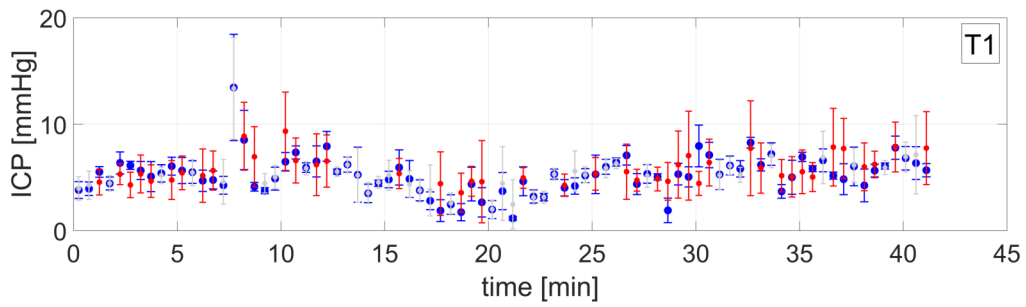


Figure S11: Time trace of the TBI subject T1. The 30 second bins are plotted with its standard deviation. The blue dots represent the ground truth (invasive ICP) while the red dots are the predicted ICP values of the validation and the light grey dots were used in the training.

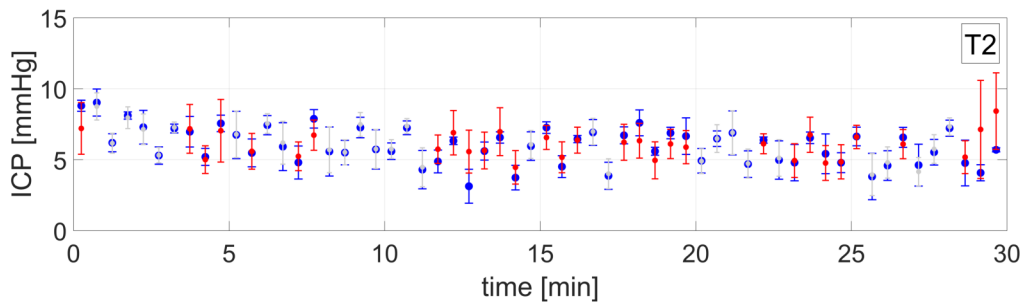


Figure S12: Time trace of the TBI subject T2. The color scheme is the same as in Figure S11.

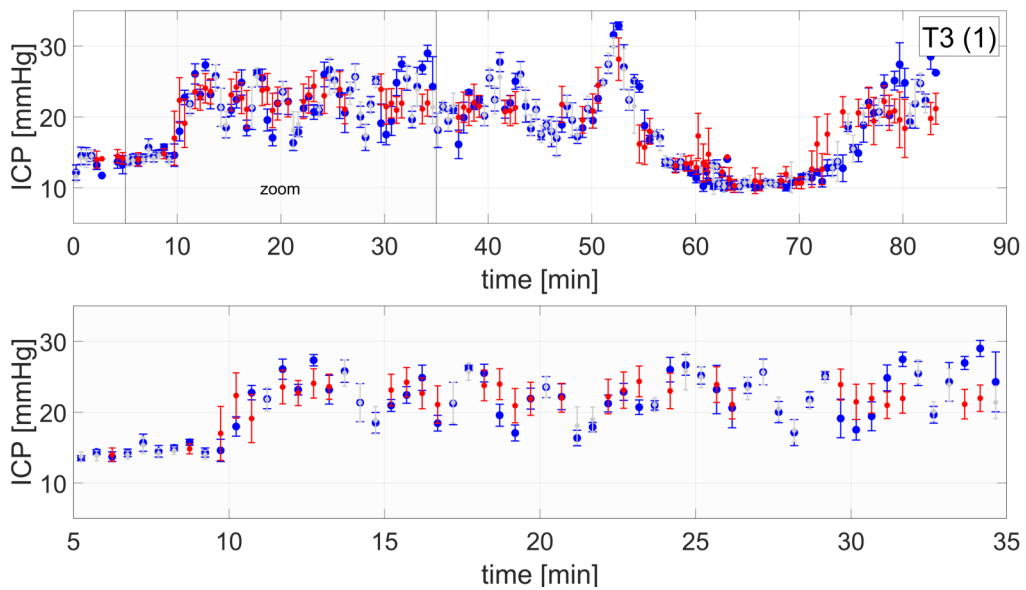


Figure S13: Time trace of the TBI subject T3 (1) with zoom showing the spontaneous increase of ICP. The color scheme is the same as in Figure S11.

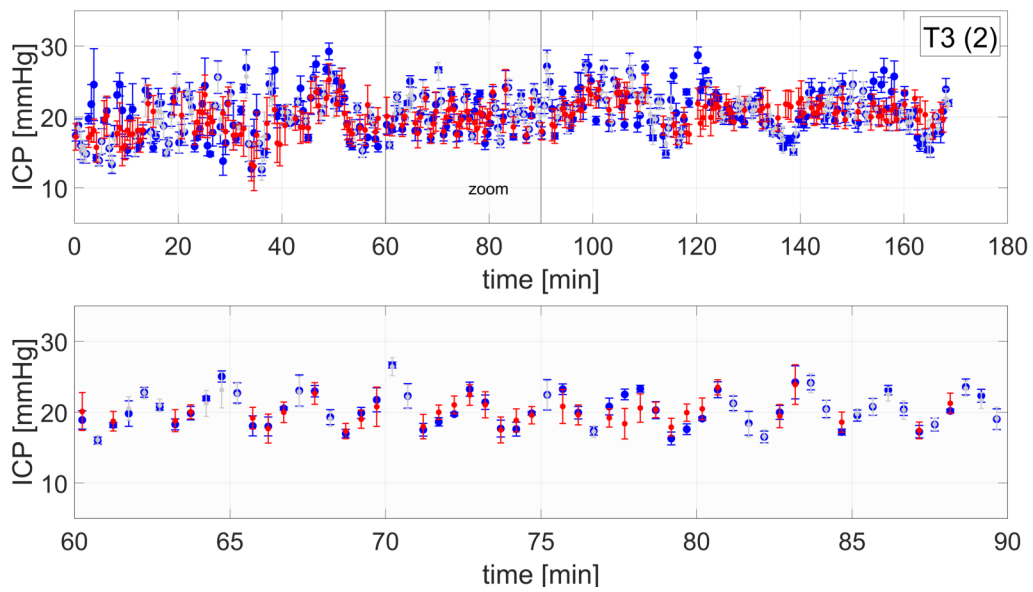


Figure S14: Time trace of the TBI subject T3 (2) with zoom for a better visualization of slow waves in the ICP time trace. The color scheme is the same as in Figure S11.

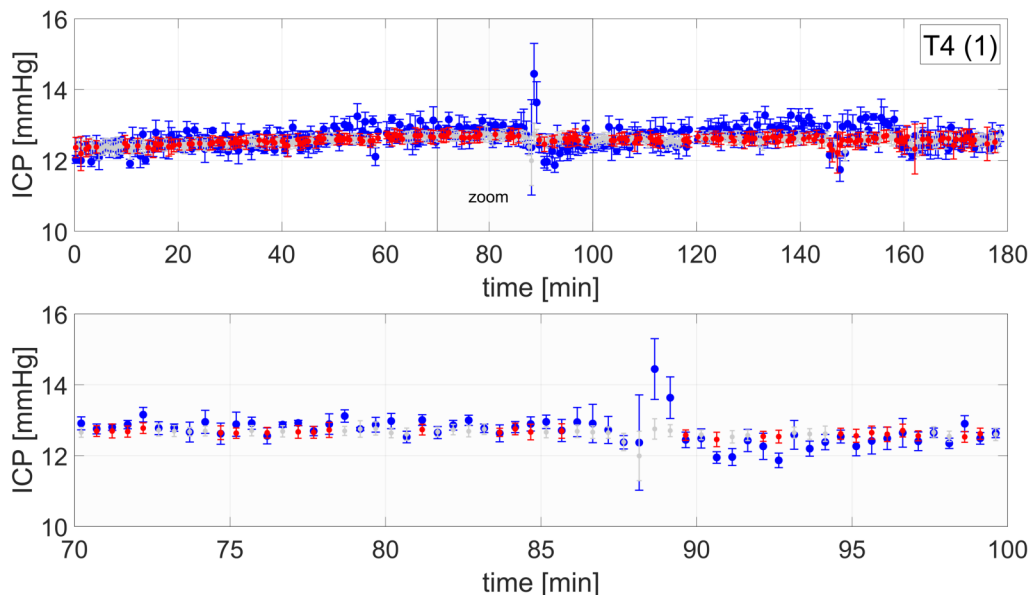


Figure S15: Time trace of the TBI subject T4 (1) with zoom. The color scheme is the same as in Figure S11.

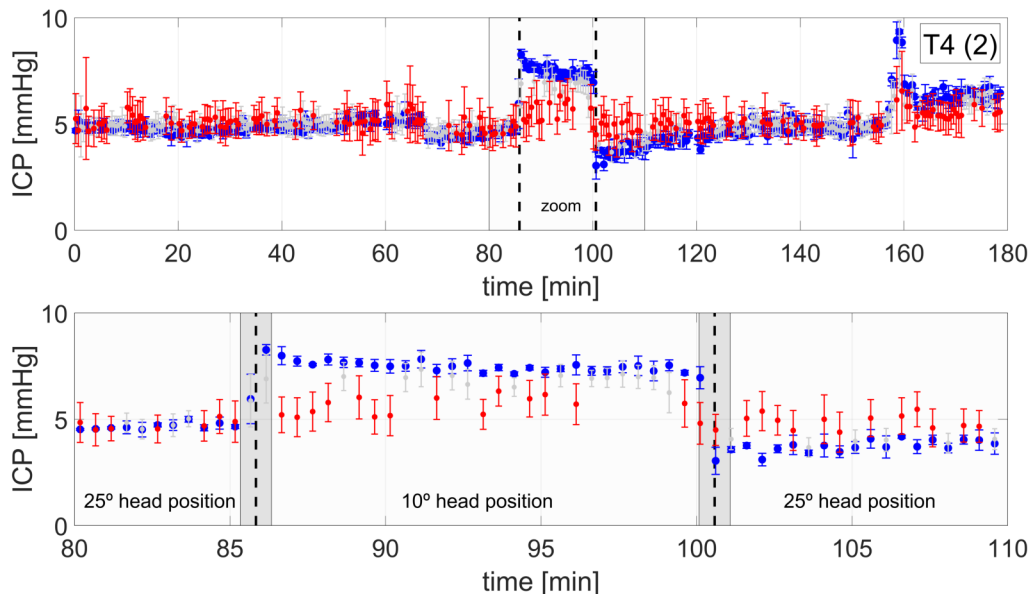


Figure S16: Time trace of the TBI subject T4 (2) with zoom showing the effect of changes in the head-of-bed position. The bed was moved within the shaded markers. The color scheme is the same as in Figure S11.

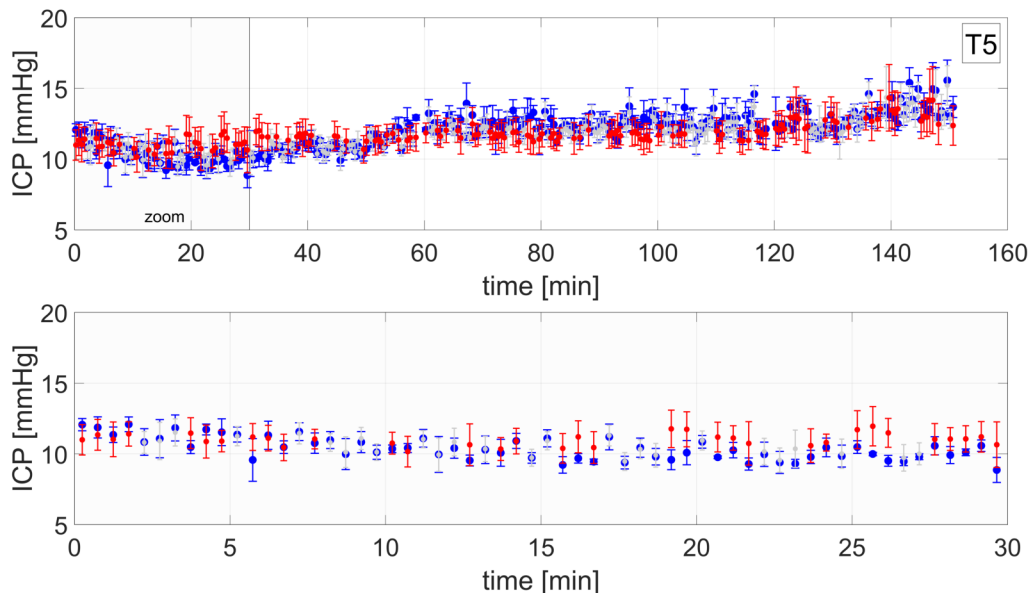


Figure S17: Time trace of the TBI subject T5 with zoom. The color scheme is the same as in Figure S11.

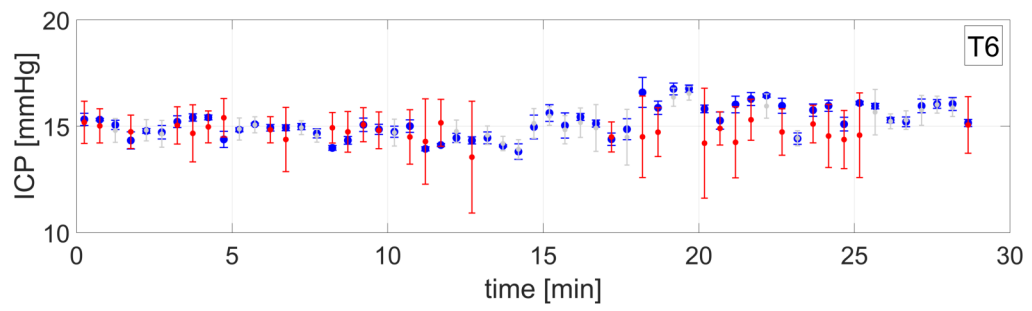


Figure S18: Time trace of the TBI subject T6. The color scheme is the same as in Figure S11.